ChemPhysChem

Research Article
doi.org/10.1002/cphc.202400582

Chemistry Europe
European Chemical Societies Publishing

www.chemphyschem.org

Quantification of the Donor-Acceptor Character of Ligands by the Effective Fragment Orbitals

Gerard Comas-Vilà[a] and Pedro Salvador*[a]

Metal-ligand interactions are at the heart of transition metal complexes. The Dewar-Chat-Duncanson model is often invoked, whereby the metal-ligand bonding is decomposed into the simultaneous ligand→metal electron donation and the metal→ligand back-donation. The separate quantification of both effects is not a trivial task, neither from experimental nor computational exercises. In this work we present the effective fragment orbitals (EFOs) and their occupations as a general procedure beyond the Kohn-Sham density functional theory (KS-DFT) framework for the identification and quantification of donor-acceptor interactions, using solely the wavefunction of the complex. Using a common Fe(II) octahedral complex framework, we quantify the σ-donor, π-donor, and π-acceptor character for a large and chemically diverse set of ligands, by introducing the respective descriptors σ^d, π^d, and π^a. We also explore the effect of the metal size, coordination number, and spin state on the donor/acceptor features. The spin-state is shown to be the most critical effect, inducing a systematic decrease of the sigma donation and π-backdonation going from low spin to high spin. Finally, we illustrate the ability of the EFOs to rationalize the Tolman electronic parameter and the trans influence in planar square complexes in terms of these new descriptors.

Introduction

Transition metal complexes stabilized by different ligands are interesting for academic research and have been used as catalysts for chemical reactions which are important for industrial purposes.[1] The chemical behavior of these complexes can be modulated by the choice of the ligands, and the understanding of the nature of these metal-ligand interactions is essential to undertake a rational design of synthetic procedures and to predict their properties. The description of the bonding in transition metal complexes is explained normally through the processes of the ligand→metal electron donation and the metal→ligand back-donation according to the Dewar-Chat-Duncanson model.[2] The donor-acceptor properties are a key point to understanding the electronic structure of the metal complexes as well as for the prediction of their stability and reactivity.[3] For this reason, different experimental and theoretical studies have been performed over the last decades in this area, although the separation of donation and backdonation effects is not so trivial. The first reliable experimental observable used to describe the electronic properties was the CO stretching frequency reported by Tolman.[4] The Tolman Electronic Parameter (TEP) is based on the position of the A_1-symmetrical ν(CO) vibration of nickel tricarbonyl complexes of the type L–Ni(CO)$_3$ with L=R$_3$P. The shift in ν(CO) is used to describe the electronic properties of L because the carbonyl ligand is sensitive to the net electron donation from the ligand to the metal atom.[5,6,7,8] Lever introduced a new parameter (Lever Electronic Parameter) based on the standard reduction potential values of Ru(III)/Ru(II) redox couple reflecting the donor capacity of ligands bound to ruthenium.[9] These electronic properties have also been estimated from NMR measures. The $^1J_{CSe}$ coupling constant for different NHC-selenium adducts has been used to predict the σ-donor strength of the respective carbenes.[10] In the same work, the ^{77}Se chemical shifts quantify the π-acidity. However, this method presents some problems. On the one hand, the signal of the carbene carbon has a very low intensity. On the other hand, the relative abundances of ^{13}C and ^{77}Se are 1.1 and 7.5% respectively. The donor strength of 10 pyrazole-derived ligands has been determined using the correlation between the donor strength of the ligand and the ^{13}C NMR chemical shift of the carbene signal suggesting an alternative to the TEP values.[11]

Despite the widespread use of the experimentally derived descriptors discussed above, there are experimental limitations such as the solubility and the toxicity of some interesting ligands. Moreover, the reliability of these descriptors to describe electron donation and back-donation fails in some cases and they are very specific. For these reasons, the theoretical methods are very helpful. Some of them have been designed to shed light on the description of the TEP, as the ones described just below, correcting the experimental drawbacks that it has.

First of all, Perrin *et al.*[12] defined a new electronic parameter (CEP) to predict the relative donor powers of ligands, calculating by DFT the ν(CO) vibration of 68 different L–Ni(CO)$_3$

[a] G. Comas-Vilà, Dr. P. Salvador
Departament de Química and Institut de Química Computacional i Catàlisi (IQCC)
Universitat de Girona
Campus Montilivi s/n 17071 Girona (Spain)
E-mail: pedro.salvador@udg.edu

Supporting information for this article is available on the WWW under https://doi.org/10.1002/cphc.202400582

complexes. The resulting ligand electronic parameter (CEP) correlated quite well with the experimental TEPs. However, this calculated parameter suffers from mode coupling and to avoid the coupling of CO stretching with other stretching, Local TEP (LTEP) has been introduced.[13] The LTEP values are based on local CO stretching force constants rather than normal mode frequencies and differ from the TEP values when describing the electronic properties of ligands L in L–Ni(CO)$_3$ complexes, especially for the carbene, halogens anions, or chalcogen-containing ligands. Recently Cremer and Kraka[14] replaced the previous LTEP with a new metal-ligand electronic parameter (MLEP), which is discussed in terms of the bond strength orders (BSOs) of the Ni–L bond. They investigated 181 L–Ni(CO)$_3$ complexes including a large variety of ligands L and concluded that the TEP is a good indicator of the metal-ligand bonding only in a few ideal cases, while the MLEP is more robust and reliable and should be better used as a reference.

Some of the theoretical methods to describe the metal-ligand bond provide a quantitative evaluation exclusively focused on the donor/acceptor properties of an isolated ligand, disregarding the potential influence from the metal-containing fragment within a given complex, for example, the analysis of the frontier orbital density and molecular electrostatic potential.[15–18] In the former the authors reported the study of eight phosphanes, using the DFT-calculated HOMO energies for the free ligands as a measure of the donor strength.[15] The proton affinities correlate well with the energy of the lone-pair at phosphorus which is the HOMO of the free phospanes. Also, the HOMO energies of different carbene ligands have been used as an indicator of the σ-donation in the works of Dong *et al.* and Ghadwal.[16,17] Moreover to demonstrate the utility of these results, the carbene ligands were used to stabilize low-valent compounds. In the latter, Suresh's molecular electrostatic potential (MESP) approach claims that the values of the molecular electrostatic potential minimum (V_{min}) corresponding to the lone pair region of substituted phosphine ligands (PR_3) are reported as a measure of the electronic effect of the PR_3 ligands. This descriptor has been calculated for 33 phosphine and phosphate ligands. The different correlations found with TEP as well as the pKa values of protonated ligands suggest that V_{min} can be used as a measure of the σ-donating ability of the phosphine. However, the back-bonding is not well accounted for with this model.[18]

In contrast, another group of theoretical methods elucidates the properties based on the whole transition metal-containing complex but requires a designated reference point which is the free fragments within their respective system geometries to determine the energy of interaction between the metal fragment and the isolated ligands. In the first step, the ligand and metal fragments are deformed into the geometry they take on in the complex from their equilibrium geometries. Next, the quasiclassical electrostatic interaction between the fragments is computed. After the antisymmetrization of the frozen fragment's reference wavefunction leads to the so-called Pauli repulsion, and the relaxation of the wavefunction to the final state leads to the orbital interaction term. This final relaxation process includes the mixing between the filled ligand orbitals and vacant metal fragment orbitals to determine the orbital interaction that can be decomposed into contributions of orbitals with different symmetry which makes it possible to distinguish between σ and π bonding.

Therefore, these methods (charge decomposition analysis (CDA),[19] energy decomposition analysis (EDA)[20,21] and the extended transition state (ETS) model)[22] rely on a priori partitioning of a complex into two (or more) fragments with predefined charges and electronic states. Subsequently, they involve a sequential calculation of the electronic structure for the fragment-donor, fragment-acceptor, and the overall complex. More recently, the metal-ligand bond has also been analyzed using the natural orbitals for chemical valence (NOCV),[23] which are defined as the eigenvectors that diagonalize the deformation density matrix which is created by subtracting the fragment's frozen reference densities from the molecular density of the complex. This leads to a very compact description of the bonding in terms of only a few orbital contributions. These methods have been used to investigate bonding in transition metal complexes.[24–30] For example, the NOCV method has been applied by Mitoraj *et al.*[24] to study the bonding between the ligands X≡CN^-, PH_3, NH_3, C_2H_4, CO, N_2, NO^+, CS, and the metal-containing fragment in the $[Ni(NH_3)_3]^{2+}$ complexes. The same authors studied in 2010 the bonding between phosphorus ligands and the metal-containing fragment [Ni(CO)$_3$], [Mo(CO)$_5$] and [Fe(CO)$_4$].[25] The analysis in both works concludes that the magnitude of donor/acceptor abilities of X are influenced by the metal-containing fragment but the relative order of the ligands remains in general intact in the phosphorous subset ligand class[25] and varies when they consider a wide range of ligands.[24]

The description of the donor/acceptor character of the N-heterocyclic carbenes (NHC)-metal bond in square-planar rhodium(I) complex (NHC)RhCl(cod) has been carried out also with the NOCV.[26] The charge-flow measured from NOCV indicated that the total back-bonding contribution is of comparable importance to donation. The EDA-NOCV results of the donor-acceptor interaction of [(L)$_2$SiC] being L=NHC^{Me}, $cAAC^{Me,}$ and PMe_3 suggest a sigma donation from the ligand to SiC fragment in the order $PMe_3 < NHC^{Me} < cAAC^{Me}$ and a π-back-donation in the same trend.[27] The analysis of the bonding between Fe(CO)$_4$ and PR_3 using the ETS method reported by Gonzalez-Blanco and Vicenç Branchadell shows that the PR_3 ligands differ mainly in the σ-donor ability, while, except for PF_3, they are all weak π-acceptors.[28] The recent work by Ardizzoia and Brenna[29] used an approach, combining the ETS method with the NOCV, to study the interaction of 41 different phosphorus ligands with the [Ni(CO)$_3$] metal fragment, highlighting the importance of metal-ligand backdonation. In 2017 Couzijn *et al.*[30] went one step forward and they applied the Hirshfeld partitioning to the resulting ETS-NOCV electronic redistributions to quantify how many electrons move from the ligand to the metal or vice versa for each bonding channel. This study comprises a wide range of ligands in various metal-carbonyl complexes and predicts that the TEP values are affected three times more strongly by σ-donation than by π-backbonding.

Another approach to quantify the donor-acceptor properties in the metal complexes is the natural bond orbital (NBO) analysis.[31] In this method, the computed wavefunction is fit to a representation of a minimum basis of natural atomic orbitals that are merged to generate the molecular bonding orbitals, while the energetic deviations from the optimal Lewis structure are determined with second-order perturbation theory. This NBO analysis, in combination with the ETS approach, has been applied to study the bonding of the $(CO)_5M\text{-}PX_3$ where X = (H, F, Me, and Cl) and M=Cr, Mo, and W in the work of Frenking *et al.*[32] suggesting that the π-bonding in the halophosphane complexes contributes 50% to the total orbital interaction. The bond between the palladium atom with the N-heterocyclic carbene in the $[PdCl_2(C_5H_5N)(C_{23}H_{40}N_4)]$ complex has also been characterized by the NBO analysis jointly with the Charge Decomposition Analysis (CDA). The results showed that the Pd atom contributes only ca. 30% to the formation of the Pd–C bond whereas the carbene carbon has a contribution of 70%. This data clearly demonstrates the strong σ-donating ability of the carbene, while the electron-deficient character of the Pd center is due to the back-donation to the carbene ligand.[33]

In this work we will show that the so-called effective fragment orbitals (EFOs),[34,35] represent a natural tool to detect *and quantify* donor-acceptor interactions. Contrary to the aforementioned approaches, our scheme does not require additional fragment (free ligand) calculations as reference. The charge and electronic state of the ligands is not imposed by the reference calculation, but it is obtained as a result of it (vide infra). It only requires the wavefunction of the complex and an underlying definition of atom within the molecule. Moreover, the EFOs can be obtained on equal footing at any level of theory (e.g. for correlated and multireference wavefunctions) as long as the density matrix is available and even in the absence of an atomic orbital basis, for instance from condensed phase calculations using plane-waves,[36] which is relevant for applications in heterogeneous catalysis.

Theory

In 1996, Mayer introduced a procedure by which the *net* density of an atom within a molecule is expressed in terms of a set of distorted (polarized) but still orthogonal effective atomic orbitals (eff-AOs) and their occupations.[34] Mayer showed that there are as many eff-AOs with significant occupation as the number of atomic orbitals in the minimal basis, thus recovering the notion of core, lone pairs, and valence atomic orbitals. In the context of Mulliken population analysis, the eff-AOs correspond to the classical natural hybrid orbitals of McWeeny, but the eff-AOs can be obtained also in the framework of real-space methods (e.g. QTAIM or overlapping atoms) or in an orthogonalized basis.

The effective fragment orbitals (EFOs) are a generalization of Mayer's eff-AOs using molecular fragments.[35] In the most general framework, the EFOs for a fragment A are obtained by diagonalizing the matrix $\mathbf{Q}^A$, with elements:

$$Q_{ij}^A = n_i^{1/2} n_j^{1/2} \int w_A^*(\vec{r}) \varphi_i^*(\vec{r}) \varphi_j(\vec{r}) w_A(\vec{r}) d\vec{r} \tag{1}$$

Here, the $\{n_i, \varphi_i(\vec{r})\}$ is the set of *m* natural orbital and natural occupations of the molecular system, and $w_A(\vec{r})$ is a weight function, fulfilling $w_A(\vec{r}) \geq 0$ and $\sum_A w_A(\vec{r}) = 1$, that accounts for the region of the space assigned to the given fragment. The fragment weight function is simply built from the contribution of the atomic weight functions of the atoms forming the molecular fragment:

$$w_A(\vec{r}) = \sum_{i \in A} w_i(\vec{r}) \tag{2}$$

Atomic weight functions can be derived from several real-space atom-in-molecule schemes such as Bader's QTAIM, Hirshfeld-type approaches, or topological fuzzy atoms (TFVC). Alternatively, a proper mapping[37] can be established to obtain the EFOs in the framework of Hilbert-space methods such as Mulliken, Löwdin or the robust natural atomic orbitals (NAO).[38]

The diagonalization of $\mathbf{Q}^A$:

$$\boldsymbol{U}^{A+} \boldsymbol{Q}^A \boldsymbol{U}^A = \boldsymbol{\Lambda}^A = diag\{\lambda_1^A, .., \lambda_m^A\} \tag{3}$$

yields ($m_A \leq m$) eigenvectors with non-zero eigenvalue, from which the orthonormalized EFOs are expressed as linear combinations of the natural/molecular orbitals truncated within the fragment domain by the corresponding weight function:

$$\chi_\mu^A(\vec{r}) = \frac{1}{\sqrt{\lambda_\mu^A}} \sum_i^m U_{i\mu}^A w_A(\vec{r}) \varphi_i(\vec{r}) \;\; \mu = \{1, .., m_A\} \tag{4}$$

The net fragment density is expressed through the EFOs and their occupations as:

$$\rho^{AA}(\vec{r}) = \sum_\mu \lambda_\mu^A \chi_\mu^{A,*}(\vec{r}) \chi_\mu^A(\vec{r}) \tag{5}$$

Hence, the occupations of the EFOs add up to the *net* fragment population.

The EFOs are the main ingredient in the effective oxidation state (EOS) analysis, a general scheme to extract oxidation states from first principles.[39] The idea is to obtain the EFOs for all fragments (in the context of coordination chemistry these are typically the transition metal centers and the ligands), sort them by decreasing occupation number, and assign electrons to the most occupied EFOs. Upon the EOS procedure, the EFOs of each fragment are formally considered either occupied or empty. To always keep the correct electron count, the EFOs of the alpha and beta parts of the density are obtained separately. In this case, the spin-resolved EFOs exhibit occupation numbers in the range $0 \leq \lambda_\mu^A \leq 1$.

The EOS procedure has been applied to a wide range of transition metal and main-group complexes, including particularly challenging systems and focusing mainly on the most

appropriate assignation of formal charges and oxidation states.[40] In the present work, we shift gears and focus instead on the actual shape of the EFOs and the relevant chemical information they can provide, in particular for the quantification of donor-acceptor properties of ligands.

Computational details

The calculations were carried out with Gaussian16.[41] All geometry optimizations were performed using the BP86 density-functional coupled with the def2tzvp basis set.[42,43] The spin resolved EFOs have been obtained with the APOST-3D program,[44] using the topological fuzzy Voronoi cells (TFVC)[45] atomic definition.

We chose as a model system a series of octahedral Fe(II) complexes $[Fe(en)(TACN)X]^{2+}$ with en = ethylenediamine and TACN = 1,4,7-Triazacyclononane. We considered a large and diverse set of up to 34 different ligands (X), depicted in Scheme 1. The set of ligands includes both anionic and neutral ligands, namely phosphines with different electronic and steric properties, Arduengo-type N-heterocyclic carbenes (NHCs),[46] and the analogs cyclic alkyl amino carbenes (cAACs),[47] or conventional carbenes (e.g. $:CF_2$ or :CFH).

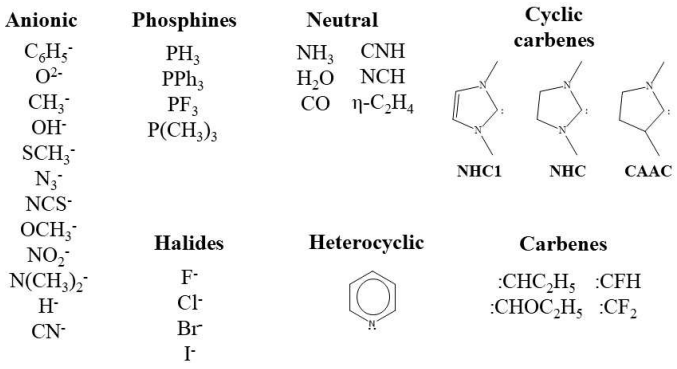

Scheme 1. Main set of ligands considered in this work.

We also include ligands interacting with the metal with different hybridizations, like sp^3 (methyl) or sp^2 (phenyl), or sp (cyanide) carbon atom or by a π system (η-C_2H_4). In addition, several typical ligands including halides, CO, pyridine, or H_2O are also included in the set.

We carried out geometry optimizations with seven different density functional theory (DFT) functionals for the $[Fe^{II}(tacn)_2](OTf)_2$·DMF and $[Fe^{II}(L)_2(en)]$ complexes (L = 2-(pyridine-2-yl)-1*H*-naphtho[2,3,*d*]imidazole-4,9-dionato),[48,49] for which accurate experimental data on bond lengths is available. A comparison of optimized Fe–N bond lengths with the experimental ones is provided in Table S1 of the SI. In general, calculated Fe–N bond lengths are somewhat too elongated compared to experiment. BP86 functional exhibited the best overall behavior and was used throughout.

Results and Discussion

Quantification of Donor/Acceptor Character of Ligands

Let us first illustrate the chemical information gathered by the EFOs taking the $[Fe(en)(TACN)CO]^{2+}$ complex as an example. The system consists of four interacting fragments, namely the Fe atom and each of the ligands. Let us focus on the obtained spin-resolved EFOs and occupations for the CO ligand, depicted in Figure 1. Because the system is described by a restricted (singlet) single-determinant wavefunction, the alpha and beta parts of the density are exactly the same, and we can focus solely on the alpha part. There are nine EFOs for CO with significant occupation numbers. There are additional EFOs with occupations below 0.01 that do have not much chemical significance. The first two EFOs, with occupation of 1.0, correspond to the 1 s core orbitals of C and O. The remaining EFOs (depicted in Figure 1 left) are in clear correspondence with

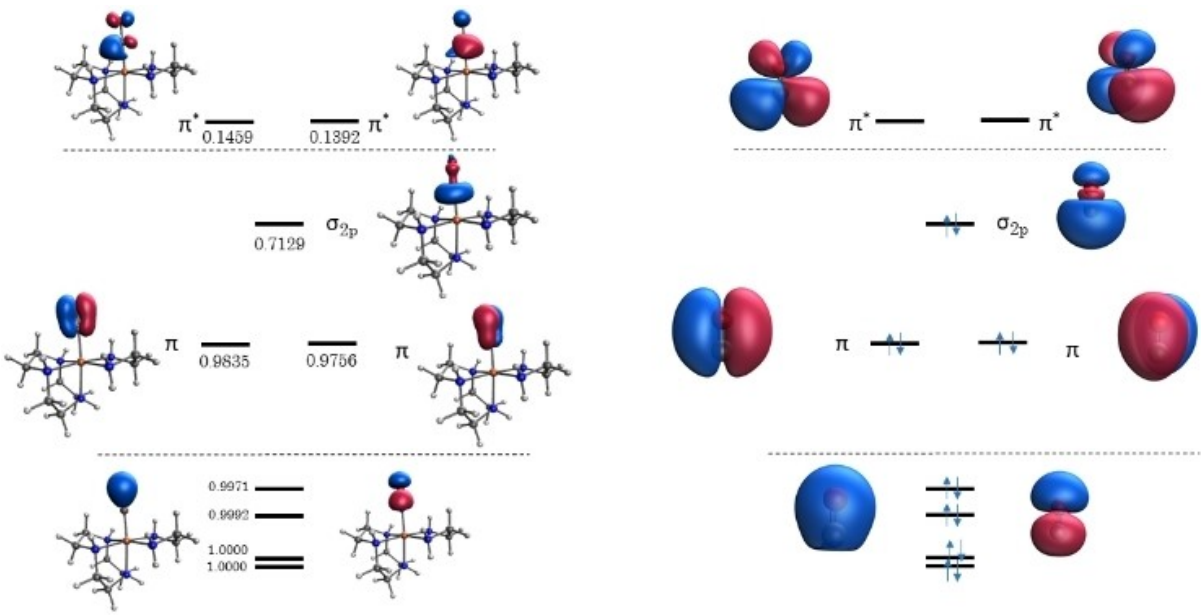

Figure 1. On the left EFOs shapes and occupancies of the CO ligand within the $[Fe(en)(TACN)CO]^{2+}$ complex and on the right the MOs of the CO molecule.

the molecular orbitals (MOs) of the *free* CO molecule, shown on the right side of Figure 1. One can identify two EFOs with occupations very close to one, that are almost indistinguishable from the σ_{2s} and σ_{2s}* inner molecular orbitals of the free CO. Then, two π-type EFOs and a σ-type EFO can also be easily put into correspondence with the degenerated π and the σ_{2pz} MOs. It is important to remark that the EFOs conform with the symmetry of the complex. Hence, even though the two π* orbitals of a free CO molecule are degenerate, the corresponding π*-type EFOs of CO *within* the complex do not have exactly the same shape and occupation number.

The shape of these EFOs is somewhat distorted compared to that of the free MOs, particularly for the σ_{2pz}-type EFO. This is because this EFO is responsible for the sigma bonding of the CO ligand with the metal, and therefore its shape is affected by both polarization from the chemical environment of the ligand within the molecule, and the truncation of the physical space, which is now shared with the Fe atom. These two effects combined result in a significant decrease of the occupation of the EFO, from the nominal value of 1 down to 0.713. This difference accounts for the *amount of sigma donation*, σ^d, from the CO ligand to the metal.

$$\sigma^d = 1 - \lambda^{\sigma,occ} \tag{6}$$

In the case of multidentate ligands, one would identify more than one σ-type EFO interacting with the metal. Then, the overall charge transferred from the ligand to the metal would be given by the sum of the contributions from all EFOs with appropriate σ symmetry.

In addition, Figure 1 also shows two additional EFOs with small but non-negligible occupations of 0.146 and 0.139. They can be put into correspondence with the *virtual* MOs of the free CO, in particular the two π* MOs. Remarkably, the virtual space of the free ligand is recovered from the occupied space of the molecule (notice only occupied MOs enter in eq. 4). In the classical DCD model, the metal-ligand interaction is completed by a backdonation from the metal into the antibonding π* orbitals of the CO, causing the well-known elongation of the C–O bond and the red-shift in the CO stretching frequency. In free CO these orbitals are empty (virtual), therefore the occupation of the corresponding EFOs can be readily seen as the amount of π donation from the metal to the ligand. The π-acceptor character of the ligand is thus given in general by:

$$\pi^a = \sum_i \lambda_i^{\pi,unocc} \tag{7}$$

where the summation runs for all formally unoccupied EFOs with the proper π symmetry.

Carbon monoxide is conventionally seen as a σ-donor π-acceptor ligand. Yet, the occupation of the two abovementioned inner π-type EFOs is not exactly 1. Similarly to eq 6, its π-donor character can also be quantified on equal footing by the deviation of the occupied EFOs of the right symmetry from its nominal value:

$$\pi^d = \sum_i (1 - \lambda_i^{\pi,occ}) \tag{8}$$

In this particular example, the molecular complex is in a singlet state, described by a restricted single determinant. This means the alpha and beta EFOs are exactly the same so that the overall charge transferred from each bonding channel is twice that given by eqns 6–8. In a more general case, one should add up the contributions coming from each spin channel.

Eqns. 6–8 can be generally used to quantify the σ-donor, π-donor, and π-acceptor character of any ligand. Notice that π-donor and π-acceptor character are not mutually exclusive, but in the light of the EFOs they co-exist, because each one is quantified using different EFOs. Ultimately, the balance between the charge donated and the charge accepted accounts for the difference between the partial charge and the formal charge (OS) of the ligand.

In fact, the difference between a π-acceptor and a π-donor ligand is given by electron count considerations or, in other words, the nature of the electronic state of the free ligand. In CO, the ligand is assumed to be neutral, so that the π* orbitals involved are nominally empty and ready to accept charge, making CO a π-acceptor. However, if we would consider the free ligand as anionic CO^{2-}, the π* orbitals would now be occupied, and the (huge) deviation from the nominal occupation would translate into π-donation.

Hence, when discussing the donor/acceptor features of the ligands it is essential to establish a reference for the electron count. Notice, however, that the EFOs in combination with EOS analysis are free from any reference state, because the occupied/unoccupied status of the EFOs is not pre-established *a priori*, but is given by the EOS procedure itself. In the case of the set of 34 ligands considered in this study, the conventional electron count and that derived from EOS analysis is the same in all cases. This, might not be the case for non-innocent ligands like NO, where the donor/acceptor characteristics of formally NO^+ and NO^- ligands will necessarily be different.

Classification of Donor/Acceptor Ligands

We performed a systematic quantification of the donor/acceptor features of the chemically diverse set of ligands gathered in Scheme 1. As a common motif, we used the octahedral Fe(II) complex $[Fe(en)(TACN)X]^{2+}$, where the *en* ligand is in an equatorial position and the X ligand is located trans to one of the coordinating N atoms of the TACN ligand. Both TACN and *en* ligands are simple, kinetically inert ligands that provide a common robust scaffold for the analysis of the electronic effect of the ligand X. We performed full geometry optimization for each complex and corroborated that they all exhibit a restricted singlet ground–state.

The shape of the EFOs obtained in each case is qualitatively analogous to those previously discussed for X=CO. There is always one occupied EFO associated with the ligand→metal σ-

donation and two pairs of unoccupied EFOs accounting for the metal→ligand π-back-donation. In addition, in most cases, there are two pairs of inner occupied π-type EFOs that can account for the ligand→metal π-donation (X=H$^-$ is an exception for obvious reasons).

Once the relevant EFOs are identified, the descriptors of eqn. 6–8 were computed, and the results obtained are displayed in Figure 2 and Tables S2–S4 of the SI.

The strongest σ-donor ligand is H$^-$, followed by most of the ligands coordinating through a carbon atom. The weakest σ-donor ligands is H_2O, followed by NH_3. F$^-$.is a stronger donor, apparently breaking the electronegativity trend. However, the formal charge of the ligands cannot be neglected and strongly influences the character of the ligand. Using X=HF as ligand the sigma donation decreases to 0.070, making it the weakest donor. On the other hand, the value for X=F$^-$ (0.290) is also smaller to that of X=OH$^-$ (0.364), and also smaller than X=NH_2^- (0.464), thus keeping the expected trends. The observed differences among different carbene or phosphine ligands indicate that it is the electronic distribution of the whole ligand that is relevant for the inductive effect, not just the nature of the contact atom.

On the other hand, π-back-bonding properties are more related to resonance effects and largely depend on the particular π electron distribution of the ligand, rather than the nature of the contact atom. The carbene ligands show strongest the π-acidity among the set, while ligands like halides, oxo, or water, not considered to be π-acceptors, show very small values of the π^a index (<0.1), as expected. Few ligands show significant values of the π^d index, indicating π-donor character. Among them one can find anionic electron-rich ligands like oxo, halides, OH$^-$, OCH_3^-, or SCH_3^-. These trends are in good agreement with the general perception of the donor/acceptor abilities of the ligands discussed in textbooks.[50]

Focusing first on the cyclic carbenes, replacing one of the nitrogen atoms in NHC with an sp^3 carbon makes the resulting cAAC carbene more π-acidic and also a better σ-donor than NHCs. In addition, the saturated NHC presents better σ-donor and π-acceptor properties than the unsaturated one (NHC1). These findings are in good agreement with the works of Dong *et al.*[16] and Ghadwal.[17] Srebro *et al.*[26] quantified the σ and charge flow using NOCV for a series of substituted NHC1 derivatives and found a significant contribution of the π-back-donation. Their reported values for the charge transfer associated with donation (0.72–0.70) and π back-donation (0.49–0.44) are somewhat larger than our σ^d (0.534) and π^a (0.270) indices, but the σ/π ratio is similar. The main conclusion regarding the cyclic carbenes is that the σ-donation is dominant, and while the π-back-donation is much smaller than for conventional linear :CR_2 carbenes, it cannot be neglected.

According to our analysis, the linear carbenes are the best σ-donors of the ligand set, only behind the hydride ligand. Moreover, the formal empty vacant p_π orbital on the contact atom makes them strong π-acceptors, showing also the largest π^a values among the set. The inclusion of an electron donating group in R induces a strong decrease in the π^a value, which goes from 0.710 in :CHC_2H_5 down to 0.484 in :$CHOC_2H_5$, because the carbon's p_π orbital is now partially occupied. This explains why alkyl carbenes are more suitable for Schrock-type carbenes, where the metal back-donation is so strong that the carbon's p_π orbital becomes actually occupied and the ligand is best described as anionic :$CHC_2H_5^-$. This is, however, not the case for our model Fe(II) system.

Phenyl and methyl ligands exhibit rather similar σ-donation, but the π-acceptor character of the former is enhanced, due to

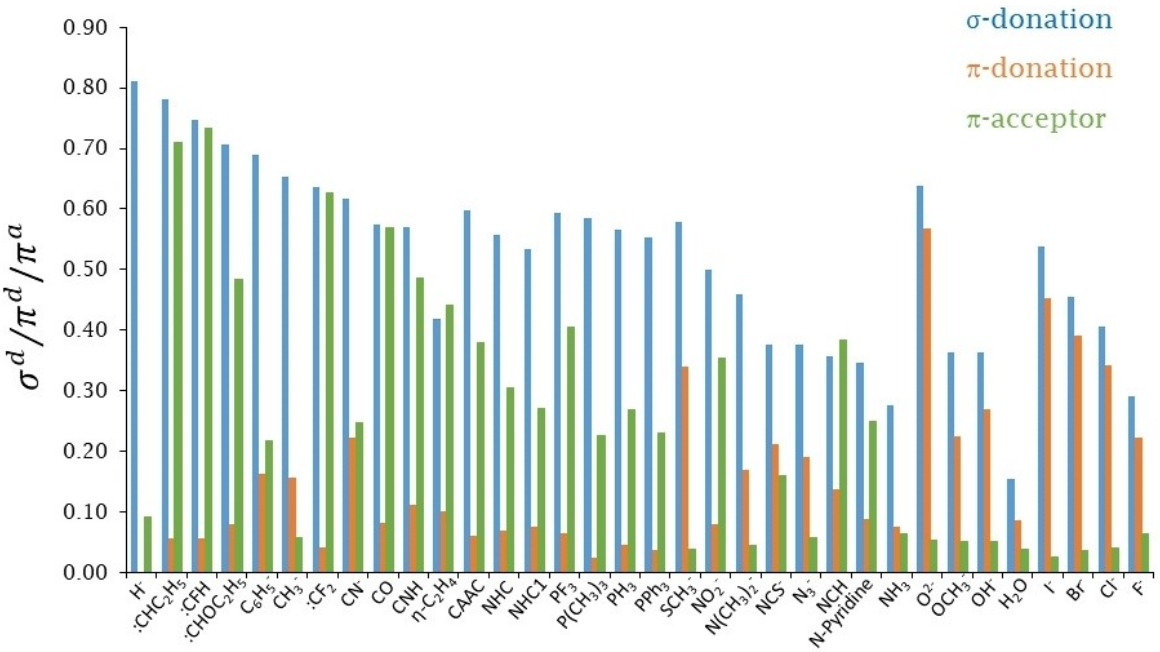

Figure 2. σ-, π-donor properties and π-acceptor properties of the X ligands in [Fe(en)(TACN)X]$^{2+}$ complexes.

the sp^2 hybridization of the unsaturated carbon contact atom. When the contact carbon atom has *sp* hybridization the π-acceptor character further increases because there is an extra electron flow channel available. However, the charge of the ligand has an important impact on the π-acceptor character. Thus, while the σ-donation of the isoelectronic CO, CNH, and CN^- is rather similar, the π^a value for CN^- is half the value for the neutral CO and CNH ligands, which show extraordinary π-acceptor properties only below the linear carbenes and over the cyclic carbenes and phosphines. Our analysis for the cyanide anion is in perfect agreement with Mitoraj et al,[24] who described it as the best σ-donor over different ligands (PH_3, NH_3, C_2H_4, and CO) and a π-acceptor character between PH_3 and NH_3 ligands.

The haptic-coordinating η-C_2H_4 ligand exhibits the smaller σ-donation among all studied carbon-based ligands. In this case, the σ-donation originates from the occupied π-system of C_2H_4. The lack of directionality and the more diffuse character of the π orbital make the σ-donation somewhat in between bromide and chloride ligands. At the same time, the availability of the unoccupied π* orbital of C_2H_4 makes it a strong π-acceptor ligand. Actually, it is the only ligand considered in this work (together with NCH) that is a better π-acceptor than σ-donor, i.e. exhibits a σ^d/π^a ratio below 1.

Phosphine ligands are another important class of ligands widely used in organometallic and coordination chemistry. We have studied four different substituted phosphines, and according to our quantitative analysis, the ordering of π-acceptor strength follows $PF_3 > PH_3 > P(Ph)_3 \geq P(CH_3)_3$. The introduction of a highly electronegative substituent like fluorine apparently facilitates the π-backdonation, which is much larger ($\pi^a = 0.404$) than for the other phosphines and even larger than for cAAC. Interestingly, the π-acidity of the primary phosphine PH_3, often used in computational models, is significantly larger ($\pi^a = 0.268$) than for the widespread tertiary phosphines. The π-acidity order of the different phosphines is in good agreement with previous theoretical estimates.[25,28,29,30,32] Originally, the π-acceptor character of the phosphines was explained by the use of high-energy d orbitals of phosphorous. Later interpretations considered instead a predominant role of antibonding σ* P–X bonds of proper π symmetry to interact with the metal. It is instructive to visualize the shape of the corresponding EFOs, depicted in Figure 3 for the $[Fe(en)(TACN)PF_3]^{2+}$ complex. Indeed, the two unoccupied EFOs with proper π symmetry are strikingly similar to the classical picture of hybridized π-acceptor orbitals of Orpen *et al.*[51] The d_{yz} and d_{xz} EFOs of the Fe also depicted in Figure 3 have the proper symmetry to feed in charge into the π-acceptor EFOs.

The mechanism of the σ donation is much simpler, governed by the EFOs on the right-hand side of Figure 3. The differences in σ-donating character of the different phosphine ligands are small, and the relative ordering varies depending on the nature of the TM and coordination number (vide infra), as also noted by Mitoraj *et al.*[25] In their paper, the authors discussed the ratio of sigma-donor/pi-acceptor strength in substituted phosphines using both energetic (using EDA/ETS),[28,32] and charge (NOCV[25]) descriptors. In Table 1 we gather

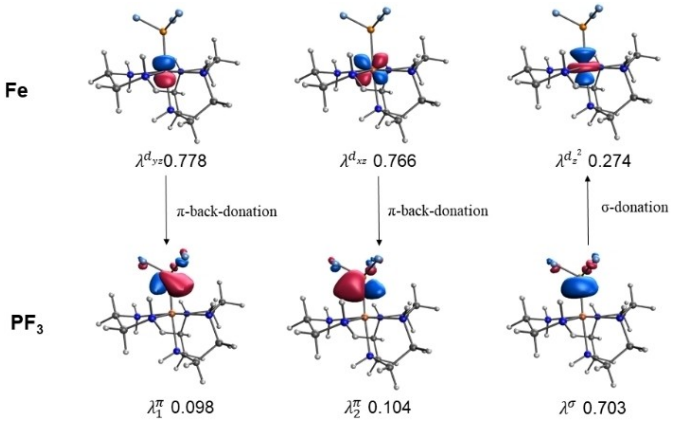

Figure 3. Shapes of the EFOs characterizing the bond between the Fe^{2+} fragment and the PF_3 ligand. The numbers denote the corresponding occupations. Only the EFOs participating in bonding are shown.

Table 1. Ratio of sigma-donor/pi-acceptor strength for phosphines $P(CH_3)_3$, PH_3, and PF_3 for different metal complexes and energetic (EDA/ETS) or charge (NOCV/EFO) descriptors.

Environment	Coord.	Method	$P(CH_3)_3$	PH_3	PF_3
$Mo(CO)_5$[32]	6	ETS	2.62	1.91	0.91
$Cr(CO)_5$[32]	6	ETS	2.89	2.21	1.03
$W(CO)_5$[32]	6	ETS	2.75	2.09	0.98
$Fe(CO)_4$[28]	5	ETS	5.82	4.31	2.10
$Mo(CO)_5$[25]	6	NOCV	1.20	1.01	0.65
$Ni(CO)_3$[25]	4	NOCV	1.24	1.00	0.59
$Fe(CO)_4$[25]	5	NOCV	1.48	1.25	0.89
$Ni(CO)_3$[29]	4	NOCV	1.25	–	0.62
$Ni(CO)_3$[30]	4	NOCV	2.14	1.52	0.87
cis-$Ir(CO)_2Cl$[30]	4	NOCV	3.50	2.33	1.37
$Fe(CO)_4$[30]	5	NOCV	2.64	1.81	1.06
$Fe(en)(TACN)^{2+}$	6	EFO	2.59	2.11	1.47

these results, including also those derived from the studies of Ardizzoia *et al.*[29] and Couzijn *et al*,[30] and our own σ^d/π^a values. As already noted by Mitoraj *et al.*,[25] the numerical values of the sigma-donor/pi-acceptor strength ratio are very different considering energetic or charge-based descriptors. We can also notice a significant effect on $Ni(CO)_3$ or $Fe(CO)_4$ frameworks using Hirshfeld-type (ref. [30]) or Lowdin-type (refs. [25] and [29]) populations in the NOCV analysis. Using Hirshfeld's populations the ratios increase and become closer to those derived from energetic descriptors. Similarly, our σ^d/π^a values are more in line with those obtained by Couzijn *et al.*[30] Nevertheless, it is interesting that, despite the different coordination and ancillary ligands, metal, and methodologies used, the relative ordering $P(CH_3)_3 > PH_3 > PF_3$ is maintained throughout. Figure S1 of the SI also shows an excellent correlation ($r^2 > 0.98$) between the ratios for $P(CH_3)_3$ and PH_3 from Table 1, demonstrating that the results obtained using the EFOs fit perfectly with other estimates.

Focusing now on the series of halide ligands, both the σ-donation and π-donation increase smoothly going down the group. The π-donation is among the largest of the set, due to the availability of lone pairs, and is comparable in magnitude with σ-donation. These results are consistent with what Frenking et al.[52] observed in the analysis of the cations AX_3^+ where A=C, Si, Ge, Sn, Pb and X=F, Cl, Br and I using NBO analysis. On the other hand, the π acceptor character, albeit very weak, exhibits the opposite trend going down the group, which further increases the net balance of π electrons.

Finally, the dianionic oxo ligand is characterized by both strong σ- and π-donation to the iron ($\sigma^d = 0.638$ and $\pi^d = 0.568$). The strong π-donating character in combination with high-valent metal species can eventually lead to metal-oxyl species.[53]

Effect of the TM, Spin State, and Coordination Number

So far, we discussed the donor-acceptor properties of the ligands in a common fixed octahedral Fe(II) framework with ancillary ligands. While the relative σ^d, π^a and π^d values described in Figure 2 are in good agreement with the literature and chemical wisdom, one should not expect a unique quantitative, universal scale of the donor/acceptor features of ligands. The formal oxidation state (or d-electron count), the size (e.g. going down the group), the coordination sphere, and the spin state of the transition metal must have some impact on the electron flow upon complex formation. While it is out of the scope of the present work to perform a fully systematic study, we have evaluated some of these effects for all the ligands. In particular, we have replaced Fe with Ru, in order to see how an increase in the metal's size (but for a fixed formal d-electron count) affects the numerical σ^d, π^d, and π^a values for the test set. The results are gathered in Tables S2–S4 of the SI. Figure 4 shows the correlation between the respective values for Fe and Ru.

We can see from thecorrelations of Figure 4 that the influence of the metal size is very small. The correlations are excellent ($r^2 > 0.96$) and the slopes are close to 1, especially for the π-donation index. In almost all cases with significant π-acceptor character, the π^a index is slightly larger for the Ru-based complexes. The mean unsigned error (MUE) for the π^a values is just 0.05, and the largest difference is found for the carbene: $CHOC_2H_5$. In the case of the σ-donation, the σ^d values systematically increase going from Fe to Ru. The MUE is again very small (0.04), but the differences in the σ^d values across different ligands are also smaller than for π^a, so some changes in the ordering of σ-donation can be observed.

For instance, in the Ru-based framework $P(CH_3)_3$ is now a slightly better σ-donor than PF_3. On the other hand, the fact that *both* π^a and σ^d values slightly increase going from Fe to Ru indicates a more covalent (less polarized) character of the M–L bonds, with EFO occupations that deviate more from the ideal 0 and 1 values for unoccupied and occupied (spin) orbitals. It is worth noticing that according to Allen's scale, Ru is less electronegative than Fe, while the opposite is predicted by Pauling's scale. Our results seem to align better with Pauling's scale.

We have also assessed the effect of the coordination number of the metal. In particular, we have considered tetrahedral iron(II) $[Fe(To^M)X]^+$ complexes, where To^M = tris(4,4-dimethyl-2-oxazolinyl)methylborate. The high-spin ($S = 2$) phenylborate derivative with X=Br^- was recently synthesized and characterized.[54] We chose this framework because it also exhibits a spectator tridentate nitrogen-based ligand. The values of the σ^d, π^d, and π^a descriptors are also gathered in Tables S2–4 of SI and the comparison with the previous results for the octahedral complex $[Fe(en)(TACN)X]^{2+}$ is shown in Figure 5.

In the tetrahedral coordination, the sigma donation is systematically smaller, as indicated by the slope > 1 in Figure 5. The MUE with respect to the octahedral coordination is again rather small (0.06) and the correlation is still quite good ($r^2 =$ 0.90). The deviations are in general much smaller for the anionic ligands. The effect on the π-acceptor character is more significant, being also reduced in the tetrahedral environment. The correlation is still good ($r^2 = 0.90$), but the MUE is larger

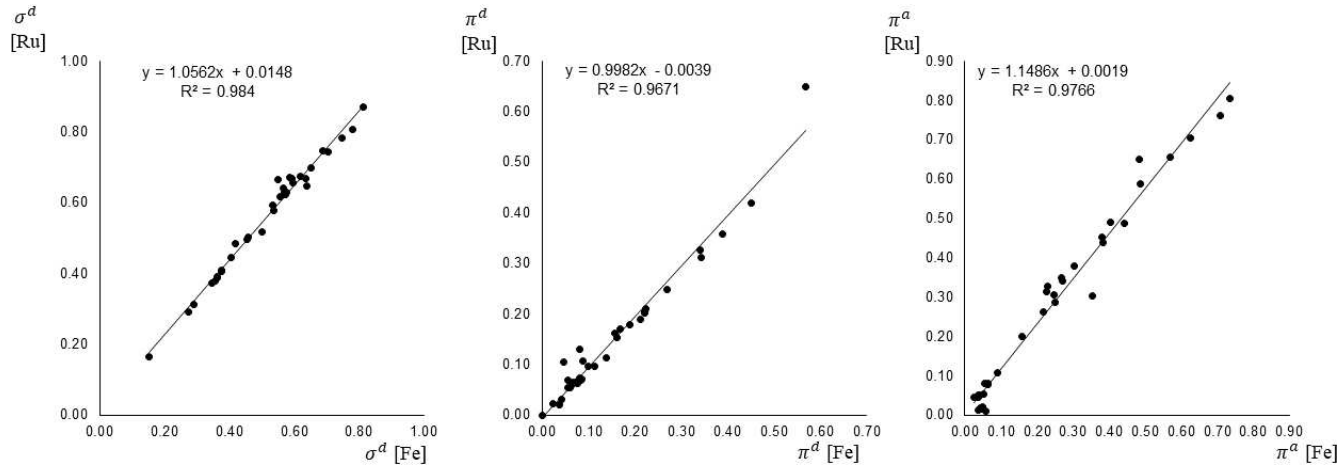

Figure 4. Comparison of σ^d, π^d, and π^a values for the ligands in $[Ru(en)(TACN)X]^{2+}$ and $[Fe(en)(TACN)X]^{2+}$ frameworks.

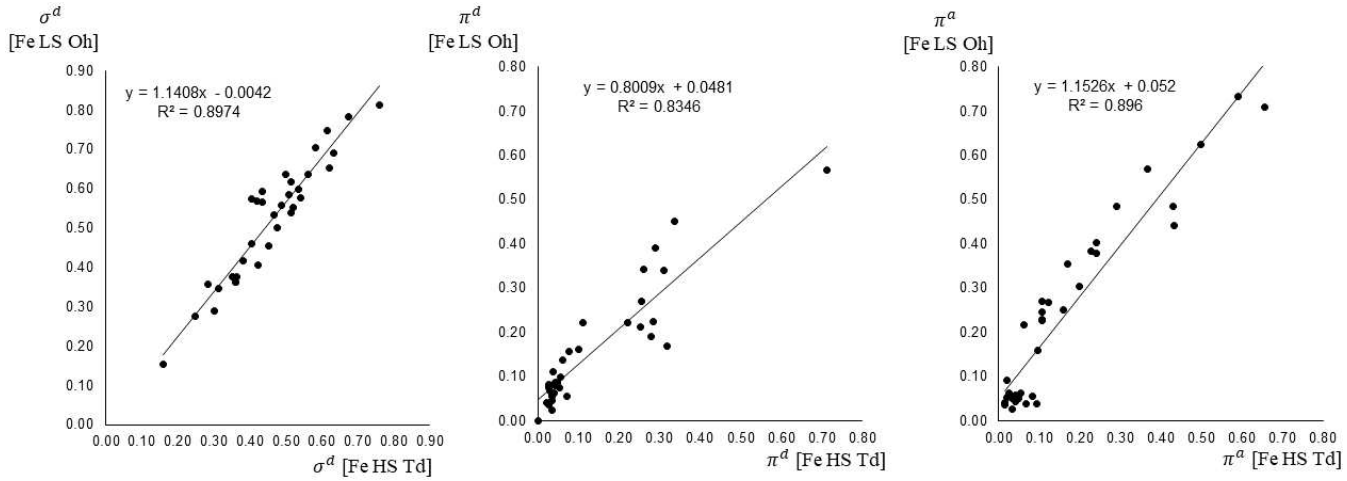

Figure 5. Comparison of σ^d, $\pi^{d,}$ and π^a values for the ligands in $[Fe(en)(TACN)X]^{2+}$ and $[Fe(To^M)X]^+$ ground-states frameworks.

(0.09) and in some cases, the deviation is important (e.g. for CO π^a goes from 0.570 to 0.366). The correlation of the π^d values is much worse, albeit the MUE remains rather small (0.05).

It is important to notice that in the tetrahedral environment, a high-spin $S=2$ ground state was found for all ligands considered. Hence, two different effects are taken into account in the comparison of Figure 5. To discern one from the other we have also considered the set of $[Fe(en)(TACN)X]^{2+}$ complexes in their high-spin $S=2$ state. The results are collected in Tables S2-S4 and Figure S2 of the SI. In the octahedral environment, going from ground-state low spin to excited-state high spin has a quite significant impact, particularly in the σ^d and π^a values, with MUE of 0.12 and 0.13, respectively. In the high-spin state, both σ^d and π^a decrease in essentially all cases, in line with a worst metal-ligand interaction, that can be also seen by larger M–X bond distances. In fact, the singlet-quintet gap can be as large as 42 kcal/mol for the :CFH ligand, so these high-lying states have little chemical relevance in the present context. However, the correlation between the high-spin $[Fe(en)(TACN)X]^{2+}$ and $[Fe(To^M)X]^+$ values is excellent (see Figure S3), with MUE values of ca. 0.04 for all three descriptors. This shows that the differences observed between $[Fe(en)(TACN)X]^{2+}$ and $[Fe(To^M)X]^+$ in their respective ground states are mostly due to the change in spin-state, rather than in the change of coordination number and symmetry.

Finally, we have also assessed the effect of using a different atom-in-molecule scheme to obtain the EFOs and their occupations. In particular, we have obtained the donor/acceptor parameters using the NAO basis, a robust Hilbert-space approach. The results for the octahedral $[Fe(en)(TACN)X]^{2+}$ complex are gathered in Tables S7-S9 and Figures S7-S9 of the SI. The σ^d and π^a parameters exhibit excellent correlations ($r^2=0.92$ and $r^2=0.94$, respectively) with those originally obtained using the real-space TFVC scheme. The σ^d values using NAO are systematically larger, and the π^a values are systematically smaller, as is evident also from the slope of the correlations. However, for the π-donating character the correlation is significantly worse ($r^2=0.71$) but, more importantly, the π^d values are very close to zero with the sole exception of the oxo ligand. The rationale behind this behaviour is that in real-space methods, each atom/fragment gathers the nearby electron density, while in Hilbert-space approaches it is the contribution of each atomic orbital that matters, regardless of whether the orbital physically extends into the domain of neighbouring atoms/fragments. Consequently, the occupation of the π-type EFOs is nearly 1 in the NAO basis because they are inner fragment orbitals. However, in the TFVC approach, these orbitals lose some density to the metal, better reflecting the π-donation.

Application of the σ^d and π^a Descriptors

As mentioned above, the Tolman electronic parameter (TEP) based on the infrared frequency of the A1-symmetrical CO stretching mode (ν_{CO}) of nickel tricarbonyl phosphine complexes $Ni(CO)_3$-L with $L{=}R_3P$ has been employed as a probe to determine the net donor power of ligand L. The rationale is that the ligand can transfer electron density to the metal, which results in an enhanced back-donation to the π* orbitals of the CO moieties, resulting in a weakening of the C–O bond and a red-shift of ν_{CO}.[4]

We have analyzed the set of $Ni(CO)_3$-PR_3 complexes reported by Ardizzoia *et al*,[29] comprising 41 different phosphine derivatives. The corresponding σ^d and π^a values for all phosphine ligands can be found in Table S5 of the SI. Considering solely the σ-donation contribution, no satisfactory correlation was found with the experimental TEP values. A much better correlation is obtained with the π^a values for the π-backdonation from the metal to the phosphine ligand (see Figure S5) so that the smaller the π-backdonation the more red-shift in the TEP values. The explanation is the more π-backbonding from the Ni to the phosphine the less π-backbonding from the metal to the CO ligands because it is a competitive effect, and consequently the stronger the C–O bonds. Figure S5 clearly shows an outlier that corresponds to

the bulky P(^{t}Bu)$_3$ ligand. In this case, the experimental TEP value exhibits the largest red shift among the set, indicating that steric factors could play an important role. The EFO occupations describe mostly electronic effects, and can only take account of steric effects in an indirect manner (e.g. changes in the geometry). Ruling out this system, the correlation found is quite good ($r^2 = 0.85$). A multiple regression analysis using σ^d and π^a descriptors leads to an improved correlation, given by eq. 9 and depicted in Figure 6:

$$TEP = -162.59\sigma^d + 297.69\pi^a + 2099.63 \; r^2 = 0.923 \quad (9)$$

Notice that the slopes of σ^d and π^a have opposite signs. Hence, larger backdonation leads to larger TEP values, but sigma donation contributes to a decrease in the TEP. This essentially means that the more electronic charge remains in the phosphine ligand, either gaining charge via enhanced backdonation or not giving away charge via decreased sigma donation, the larger the TEP value. Indeed, Figure S7 shows a very good correlation between the experimental TEP value and simply the partial charge on the phosphine ligand ($r^2 = 0.88$) excluding again the P(^{t}Bu)$_3$ outlier. In the original study of Ardizzoia *et al*,[29] the authors relied upon ETS-NOCV charge descriptors, that included sigma donation, pi backdonation but also sigma-backdonation from the metal to the phosphine. The authors concluded that this σ-backdonation plays a decisive role in explaining the experimental TEP values. The σ-backdonation in ETS-NOCV calculations is controversial, and can sometimes be associated with the way the fragment's reference states are constructed. Our analysis using the EFOs and their occupations shows quite similar performance without resorting to additional fragment reference state calculations.

Finally, we also tackle the trans influence, which is the substituent effect of a ligand on the metal-ligand bond trans to it.[55–59] This influence has been commonly represented by square planar complexes with a d^8 metal configuration and it is basically measured by the metal-ligand bond lengths trans to a particular ligand.[60–62]

We have studied the trans influence from the set of 33 square-planar metal carbonyl species of general formula cis-[Rh^I(CO)(Cl)(L)$_2$], collected by Fusè *et al*.[63] We have computed the σ^d and π^a descriptors for the ligand L, in position trans to the CO, and analyzed their relationship with the equilibrium Rh–C bond lengths. The corresponding results can be found in Table S6 of the SI. The Rh–C distances range between 1.764 Å and 1.913 Å, so the Rh–C bond trans to PF_3 is ca. 0.15 Å longer than the Rh–C bond trans to F^-, indicating quite significant trans influence. Remarkably, the largest π^a value among the set is obtained for the halogenated phosphine PF_3 ($\pi^a = 0.278$), whereas the halogen F^- ligand exhibits the smallest one ($\pi^a = 0.040$). Thus, the better π-acceptor the ligand is, the weaker the metal-ligand bond trans to it. Figure 7 shows the correlation between the calculated equilibrium Rh–C bond lengths and the π^a properties of the ligands L. The good correlation obtained ($r^2 = 0.914$) strongly suggests π^a as a quantitative descriptor of the trans influence. We can understand this behavior as a competition between the ligands in the trans position to accept π density from the metal. Thus, the strong π-accepting ligands such as PF_3 reduce the capacity of the CO ligand to get this π density (π^a CO = 0.408). In contrast, weak π-accepting ligands such as F^- increase the ability of the CO ligand to accept this π density (π^a CO = 0.844), the bond becomes stronger, and the Rh–C is shorter.

On the other hand, the σ donor ability of the X ligand correlates only poorly with the Rh–C bond length (Figure S8,

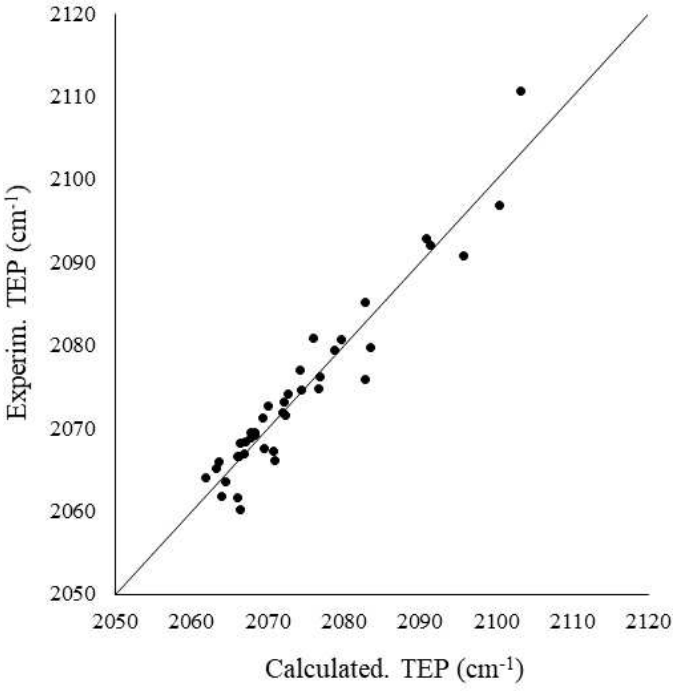

Figure 6. Linear relationship between the experimentally TEP (cm^{-1}) and the parametrization obtained with π-acceptor properties and the σ-donation properties of the different PR_3 ligands excluding the P(^{t}Bu)$_3$ outlier.

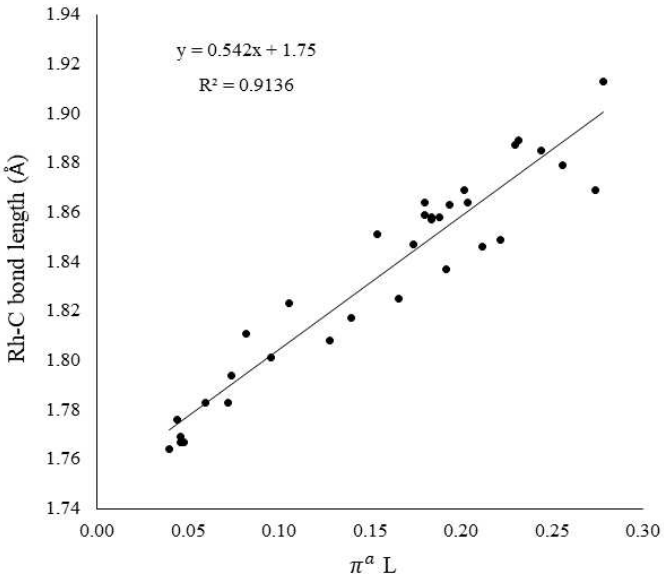

Figure 7. Correlation between π^a of the L ligand and the Rh–C bond length for the set of cis-[Rh^I(CO)(Cl)(L)$_2$] complexes.

$r^2 = 0.546$). Including both σ^d and π^a descriptors in a multilinear regression leads to eq. 10.

$$Rh{-}C_{bond\ length} = 0.087\sigma^d + 0.454\pi^a + 1.725\ r^2 = 0.957 \quad (10)$$

The coefficient for σ^d is very small, indicating that the main role is played by the π-acceptor features, as could be expected. Still, the results indicate that the larger the sigma donation by the L ligand, the more trans influence. This inductive effect is translated into differences in σ^d values of the CO ligand trans to L. For the best σ-donor ligand, $P(OMe)_3$, $\sigma^d = 0.612$ and the σ^d value for the trans CO ligand is 0.576. Conversely, for the weakest σ-donor ligand, H_2O, $\sigma^d = 0.196$, and the σ^d value for the trans CO ligand increase to 0.717.

These different values of σ^d for the same CO ligand illustrate once again that the donor/acceptor features of the ligands are not expected to be fixed but vary according to the chemical environment they experience. We show that these sometimes subtle differences can be readily captured by the occupation of the corresponding EFOs highlighting their relevance in the rationalization and quantification of metal-ligand interactions.

Conclusions

We have shown that the effective fragment orbitals (EFOs) and their occupations represent a versatile tool offering a wave-function-based approach for characterizing donor-acceptor interactions without recurring to additional fragment reference calculations. Utilizing a simple Fe(II) octahedral complex model, we have successfully identified and quantified sigma-donor, pi-donor, and pi-acceptor traits across a chemically diverse set of ligands, by introducing simple and intuitive descriptors based on the occupation of the relevant EFOs of the ligand, namely σ^d, π^d, and π^a for sigma and pi donation and for pi-acceptor character, respectively. The relative ordering of the donor/acceptor features is in line with other computational estimates and in good agreement with chemical intuition. Notably, spin state emerges as the most relevant effect, systematically decreasing the amount of sigma-donation and pi-backdonation from low to high spin configurations. Moreover, we demonstrate the efficacy of EFOs in elucidating Tolman electronic parameters and the trans-influence phenomena in planar square complexes through these descriptors.

Supporting Information

Additional Tables and Figures and XYZ coordinates of all optimized complexes.

Acknowledgements

This research was funded by the Ministerio de Ciencia, Innovación y Universidades (MCIU), grant number PID2022-140666NB-C22. G.C. also acknowledges support from FPU grant 19/02781.

Conflict of Interests

The authors declare no conflict of interest.

Data Availability Statement

The data that support the findings of this study are available in the supplementary material of this article.

Keywords: chemical bonding · chemical concepts · wavefunction analysis · donor-acceptor interactions · transition metal complexes

[1] A. D. Ketley, F. X. Werber, *Science* **1964**, *145*, 667–673.
[2] J. Chatt, L. A. Duncanson, *J. Chem. Soc.* **1953**, 2939–2947.
[3] G. Frenking, N. Fröhlich, *Chem. Rev.* **2000**, *100*, 717–774.
[4] C. A. Tolman, *Chem. Rev.* **1977**, *77*, 313–348.
[5] L. E. Orgel, *Inorg. Chem.* **1962**, *1*, 25–29.
[6] F. A. Cotton, *Inorg. Chem.* **1964**, *3*, 702–711.
[7] G. Bistoni, S. Rampino, N. Scafuri, G. Ciancaleoni, D. Zuccaccia, L. Belpassi, F. Tarantelli, *Chem. Sci.* **2016**, *7*, 1174–1184.
[8] D. Sorbelli, L. Belpassi, F. Tarantelli, P. Belanzoni, *Inorg. Chem.* **2018**, *57*, 6161–6175.
[9] R. A. Metcalfe, A. B. P. Lever, *Inorg. Chem.* **1997**, *36*, 4762–4771.
[10] K. Verlinden, H. Buhl, W. Frank, C. Ganter, *Eur. J. Inorg. Chem.* **2015**, *2015*, 2416–2425.
[11] J. C. Bernhammer, H. V. Huynh, *Dalton Trans.* **2012**, *41*, 8600–8608.
[12] L. Perrin, E. Clot, O. Eisenstein, J. Loch, R. H. Crabtree, *Inorg. Chem.* **2001**, *40*, 5806–5811.
[13] R. Kalescky, E. Kraka, D. Cremer, *Inorg. Chem.* **2013**, *53*, 478–495.
[14] D. Setiawan, R. Kalescky, E. Kraka, D. Cremer, *Inorg. Chem.* **2016**, *55*, 2332–2344.
[15] H. M. Senn, D. V. Deubel, P. E. Blöchl, A. Togni, G. Frenking, *J. Mol. Struct.* **2000**, *506*, 233–242.
[16] Z. Dong, J. T. Blaskovits, F. Fadaei-Tirani, R. Scopelliti, A. Sienkiewicz, C. Corminboeuf, K. Severin, *Chem. Eur. J.* **2021**, *27*, 11983–11988.
[17] R. S. Ghadwal, *Acc. Chem. Res.* **2022**. *55*, 457–470.
[18] C. H. Suresh, N. Koga, *Inorg. Chem.* **2002**, *41*, 1573–1578.
[19] S. Dapprich, G. Frenking, *J. Phys. Chem.* **1995**, *99*, 9352–9362.
[20] K. Kitaura, K. Morokuma, *Int. J. Quantum Chem.* **1976**, *10*, 325–340.
[21] K. Kitaura, S. Sakaki, K. Morokuma, *Inorg. Chem.* **1981**, *20*, 2292–2297.
[22] T. Ziegler, A. Rauk, *Theor. Chim. Acta* **1977**, *46*, 1–10.
[23] M. P. Mitoraj, A. Michalak, *J. Mol. Model.* **2007**, *13*, 347–355.
[24] M. P. Mitoraj, A. Michalak, *Organometallics* **2007**, *26*, 6576–6580.
[25] M. P. Mitoraj, A. Michalak, *Inorg. Chem.* **2010**, *49*, 578–582.
[26] M. Srebro, A. Michalak, *Inorg. Chem.* **2009**, *48*, 5361–5369.
[27] D. M. Andrada, G. Frenking, *Angew. Chem. Int. Ed.* **2015**, *54*, 12319–12324.
[28] O. Gonzáles-Blanco, V. Branchadell, *Organometallics* **1997**, *16*, 5556–5562.
[29] G. Attilio Ardizzoia, S. Brenna, *Phys. Chem. Chem. Phys.* **2017**, *19*, 5971–5978.
[30] E. P. A. Couzijn, Y. Y. Lai, A. Limacher, P. Chen, *Organometallics* **2017**, *36*, 3205–3214.
[31] A. E. Reed, L. A. Curtiss, F. Weinhold, *Chem. Rev.* **1988**, *88*, 899–926.
[32] G. Frenking, K. Wichmann, N. Fröhlich, J. Grobe, W. Golla, D. L. Van, B. Krebs, M. Läge, *Organometallics* **2002**, *21*, 2921–2930.
[33] H. Karabıyık, B. Yiğit, M. Yiğit, İ. Özdemir, H. Karabıyık, *Acta Crystallogr.* **2019**, *75*, 941–950.
[34] Mayer, *J. Phys. Chem.* **1996**, *100*, 6249.
[35] E. Ramos-Cordoba, P. Salvador, I. Mayer, *J. Chem. Phys.* **2013**, *138*, 214107.
[36] I Mayer, I Bako, A Stirling, J . *Phys. Chem. A* **2011**, *115*, 12733–12737.

[37] P. Salvador, *Exploring Chemical Concepts Through Theory and Computation*, John Wiley & Sons **2024**, p 207.
[38] A. E. Reed, F. Weinhold, *J. Chem. Phys.* **1983**, *78*, 4066–4073.
[39] E. Ramos-Cordoba, V. Postils, P. Salvador, *J. Chem. Theory Comput.* **2015**, *11*, 1501.
[40] V. Postils, C. Delgado-Alonso, J. M. Luis, P. Salvador, *Angew. Chem. Int. Ed.* **2018**, *57*, 10525.
[41] M. J. Frisch, et al., *GAUSSIAN 16 (Revision C.01.)*, Gaussian, Inc., Wallingford, CT, **2016**.
[42] A. D. Becke, *Phys. Rev.* **1988**, *38*, 3098–3100.
[43] J. P. Perdew, *Phys. Rev.* **1986**, *34*, 8822–8824.
[44] P. Salvador, E. Ramos-Cordoba, M. Montilla, L. Pujal, M. Gimferrer, *J. Chem. Phys.* **2024**, *160*, 172502.
[45] P. Salvador, E. Ramos-Cordoba, *J. Chem. Phys.* **2013**, *139*, 071103.
[46] R. Jazzar, M. Soleilhavoup, G. Bertrand, *Chem. Rev.* **2020**, *120*, 4141–4168.
[47] S. Kundu, S. Sinhababu, V. Chandrasekhar, H. W. Roesky, *Chem. Sci.* **2019**, *10*, 4727–4741.
[48] A. S. Tolla, A. Banerjee, S. Stjepanovic, J. Li, W. W. Brennessel, R. Loloee, F. A. Chavez, *Eur. J. Inorg. Chem.* **2013**, *12*, 2115–2121.
[49] T. Shiga, R. Kumamaru, G. N. Newton, H. Oshio, *Dalton Trans.* **2020**, *49*, 1485–1491.
[50] D. F. Shriver, P. W. Atkins, C. H. Langford, *Inorganic Chemistry*, Oxford University Press: Oxford, England, **1990**.
[51] A. Guy Orpen, N. G. Connelly, *Organometallics* **1990**, *9*, 1206–1210.
[52] G. Frenking, S. Fau, C. M. Marchand, H. Grützmacher, *J. Am. Chem. Soc.* **1997**, *119*, 6648–6655.
[53] Y. Shimoyama, T. Kojima, *Inorg. Chem.* **2019**, *58* (15), 9517–9542.
[54] R. R. Reinig, A. Ellern, A. D. Sadow, *Inorg. Chem.* **2019**, *58*, 6044–6051.
[55] J. Cooper, T. Ziegler, *Inorg. Chem.* **2002**, *41*, 6614–6622.
[56] P. N. Kapoor, R. Kakkar, *J. Mol. Struct.* **2004**, *679*, 149–156.
[57] P. K. Sajith, C. H. Suresh, *J. Organomet. Chem.* **2011**, *696*, 2086–2092.
[58] Z. Chval, M. Sip, J. V. Burda, *J. Comput. Chem.* **2008**, *29*, 2370–2381.
[59] F. Guégan, V. Tognetti, L. Joubert, H. Chermette, D. Luneau, C. Morell, *Phys. Chem. Chem. Phys.* **2016**, *18*, 982–990.
[60] Y. Zhang, Z. Guo, X. Z. You, *J. Am. Chem. Soc.* **2001**, *123*, 9378–9387.
[61] P. Carloni, M. Sprik, W. Andreoni, *J. Phys. Chem.* **2000**, *104*, 823–835.
[62] S. Dasari, P. Bernard Tchounwou, *Eur. J. Pharmacol.* **2014**, *740*, 364–378.
[63] M. Fusé, I. Rimoldi, G. Facchetti, S. Rampino, V. Barone, *Chem. Commun.* **2018**, *54*, 2397–2400.

Manuscript received: May 23, 2024
Accepted manuscript online: June 4, 2024
Version of record online: ■■, ■■

RESEARCH ARTICLE

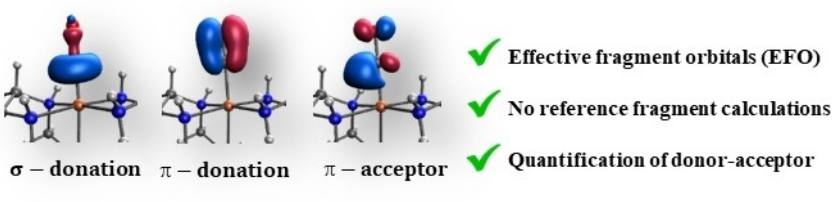

*G. Comas-Vilà, Dr. P. Salvador**

1 – 13

Quantification of the Donor-Acceptor Character of Ligands by the Effective Fragment Orbitals

The effective fragment orbitals and their occupations are used to quantify the donor-acceptor properties of ligands. They can be obtained for general wavefunctions and without reference fragment calculations.

Quantitative indices for sigma donation (σ^d), pi donation (π^d) and pi-acceptor character (π^a) are introduced and evaluated for a chemically diverse set of ligands.